Effects of Various Suspended Mounting Schemes on Mode Characteristics of Coupled Slotlines Considering Conductor Thickness for Wideband MIC Applications

Tongqing Wang and Ke Wu, *Senior Member, IEEE*

***Abstract*—Propagation characteristics of fundamental and higher-order modes are determined in coupled slotlines with three suspended mounting schemes (pedestal, groove, inverse pedestal) for wideband applications of microwave and millimeter-wave integrated circuits. The analysis is based on a novel enhanced spectral domain approach (ESDA) that combines essentially the conventional spectral domain technique with the power conservation theorem. Numerical results, considering also the influence of finite conductor thickness, are presented for propagation constants and characteristic impedance of the fundamental modes. Effects of different suspended mounting schemes on cutoff frequencies of first higher-order even and odd modes are discussed in detail. Field profiles of the fundamental modes in coupled slotlines with and without pedestals are shown. The inherent mechanism of mode transition is explained with respect to different pedestal sizes, indicating that the monomode bandwidth can be extended by appropriately choosing the dimension of pedestal in coupled slotlines.**

I. Introduction

OVER the last decade, coplanar-type transmission lines have widely been used in microwave and millimeter-wave hybrid and monolithic integrated circuits as an alternative to microstrip lines. Parallelly, various slotlines including coupled geometry become fundamental transmission media in miniature planar MIC's. Compared to the microstrip line, the main advantages of these lines are that they allow easy implementation of active and passive devices both in series and shunt connections, thereby eliminating the need for via holes and thin substrate, and thus simplifying the fabrication process, as well as permitting direct on-wafer measurements. It is also possible to reduces the parasitic inductance due to the grounded three-terminal devices. In addition, it offers low dispersion and additional degree of freedom for a wide range of characteristic impedance [1], [2].

Coplanar waveguide is considered as a special coupled slotline in which the odd mode (with respect to the currents on two side planes) is suppressed. Recent theoretical investigation on coplanar structures is essentially focused on propagation characteristics and discontinuities [2]–[6]. In practice, a coplanar microwave and millimeter-wave integrated circuit is usually placed on a metallic plane for mechanical support, thus forming a conductor-backed topology. This structure suffers from potential problem of leakage and mode conversion due to interaction among various modes [7], [8]. Apart from causing an energy loss of the fundamental mode, the leaky power may be coupled with other parts of the circuit, producing some unexpected electrical effects. Electrical performance of the conductor-backed coplanar waveguides (CBCPW's) has been studied by a number of researchers. An integral equation technique was used to determine the possible mode conversion at the open end in finite-width CBCPW's [9]. High-order modes profiles for the CBCPW's with bilaterally shielded via-holes were shown and the possible monomode bandwidth was assessed theoretically and confirmed experimentally in [10]. Resonant phenomena in CBCPW's have been also analyzed theoretically and experimentally in [11]. These drawbacks, which deteriorate electrical performance of the CPW structures at higher frequency, can be eliminated by suspended mounting

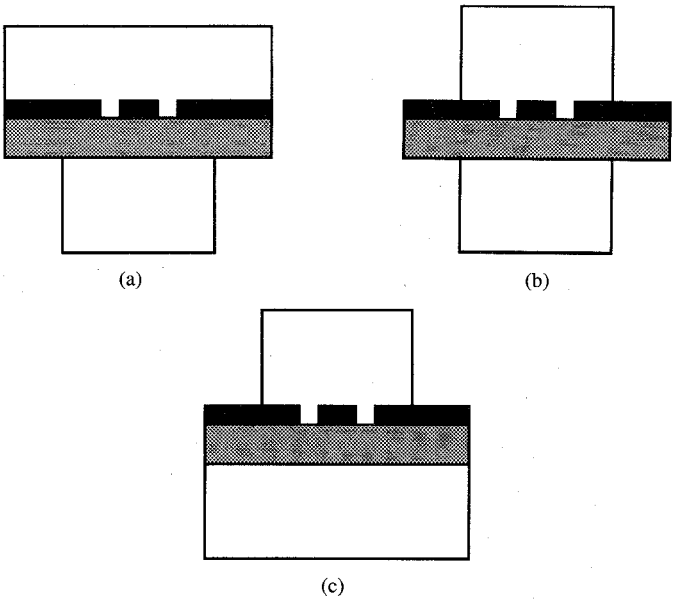

Fig. 1. Coupled slotlines with various suspended mountings: (a) pedestal; (b) groove; and (c) inverse pedestal.

Manuscript received April 4, 1994; revised July 1, 1994. This work was supported by Natural Science and Engineering Research Council (NSERC) of Canada.

The authors are with the Groupe de Recherches Avancées en Microondes et en Électronique Spatiale, (POLY-GRAMES), Dept. de génie électrique et de génie informatique, École Polytechnique, Montréal H3C 3A7, Canada.

IEEE Log Number 9410335.

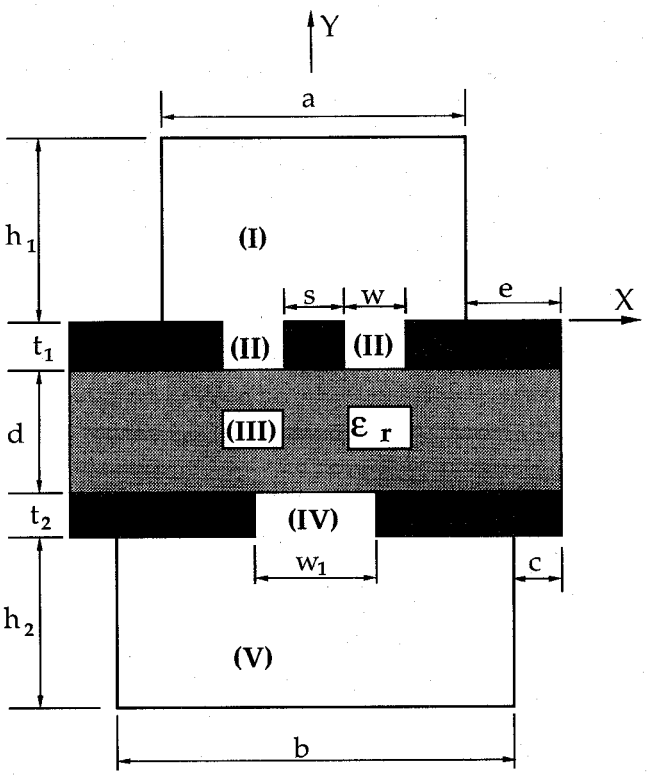

Fig. 2. Generalized coupled slotline with septum.

in a shielded rectangular box. In suspended coplanar structure, however, the mounting grooves are usually required. As pointed out in [12]–[14], the structure with mounting grooves has some intrinsic disadvantages. The mounting grooves make the monomode bandwidth significantly decreased. On the other hand, electrical isolation and grounding are affected due to the split housing. The precise machining of the housing is needed to ensure that the dielectric is properly supported. Note that this kind of structure is not well suited for applications in today's fast developed MMIC technology because the GaAs substrate is relatively thin and fragile.

In order to preserve the advantages of the housing and overcome these shortcomings, two novel mounting strategies with pedestal and inverse pedestal are proposed in this paper as shown in Fig. 1. From the viewpoint of numerical analysis, a general structure illustrated in Fig. 2 is considered. In order to increase certain degree of freedom in design aspects, the septum located at the other side of substrate is introduced. Obviously, the structure of Fig. 2 includes all three structures of Fig. 1 that consider also the finite thickness of planar conductors. The electrical effect of the finite conductor thickness may be significant at millimeter-wave frequencies, which will be incorporated in the following analysis.

The coupled slotline structure shown in Fig. 2 is quite complicated. Therefore, accurate full-wave analysis of its propagation characteristics is the key to its successful practical applications. Although different numerical techniques for solving guided-wave characteristics of these structures have recently been proposed, most of them usually present a compromise between accuracy and efficiency of numerical results as well as application range. In this work, a novel enhanced spectral-domain approach is developed to determine propagation characteristics of the structure as shown in Fig. 2. Compared to the conventional and other modified SDA, the proposed technique is more efficient in terms of analytical effort and numerical accuracy. This is done by avoiding usually lengthy derivation of the Green's function matrix for complex structures. In addition, this technique features an independent choice of truncated spectral terms in each subregion. Therefore, this method is in particular suitable for the analysis of structures containing large ratio of lateral widths in adjacent subregions. This is the unmatched advantage over the mode-matching method in solving the same problems. The method is general and easy to handle for programming.

In this paper, numerical results are presented for propagation constants and characteristic impedance of the fundamental modes. Effects of different suspended mounting schemes on cutoff frequencies of first higher-order even- and odd-modes are discussed. Field profiles are shown in an effort to understand better the propagation mechanism of coupled slotlines with pedestal. Mode transition in coupled slotlines against different pedestal sizes is also explained in detail.

II. Theory

The enhanced SDA is based on a strategy of combining conventional SDA with power conservation theorem. More precisely, tangential magnetic field at both boundaries of each stratified subregion (homogeneous dielectric layer) can be expressed in terms of its electric counterpart. On the other hand, the boundary conditions at the interfaces are satisfied by imposing power conservation theorem in the space domain. A detailed description of the newly developed method for analysis of generalized planar structures will be presented somewhere else [15]. Therefore, only some highlights are outlined here. At first, as usually done in spectral domain analysis, all conductors are assumed to be electrically perfect. In Fig. 2, the whole structure may be divided into five homogeneous rectangular subregions which are interconnected to each other and bounded by lateral conducting walls. Electromagnetic fields in each subregion can be expanded in the spectral domain, such as

$$\begin{pmatrix}\vec{E}\\ \vec{H}\end{pmatrix}^i = \sum_{n=-\infty}^{+\infty} \begin{pmatrix}\tilde{\vec{E}}(y)\\ \tilde{\vec{H}}(y)\end{pmatrix}_n^i \cdot e^{-j(\alpha_n^i \cdot x + \beta \cdot z)} \tag{1}$$

where

$$\begin{pmatrix}\tilde{\vec{E}}(y)\\ \tilde{\vec{H}}(y)\end{pmatrix}_n^i = \frac{1}{a_i}\int_{a_i} \begin{pmatrix}\vec{E}\\ \vec{H}\end{pmatrix}^i \cdot e^{j(\alpha_n^i \cdot x + \beta \cdot z)} \cdot dx \tag{2}$$

and

$$\alpha_n^i = \begin{cases} \dfrac{(2n-1)\pi}{a_i} & \text{for even-mode} \\ \dfrac{2n\pi}{a_i} & \text{for odd-mode} \end{cases} \tag{3}$$

(n) refers to the spectral term; a_i is the width of all possible subregions $(a, w, a+2e, w_1, b)$; and (i) stands for the subregions (I, II, III, IV, V). Note that the even and odd field

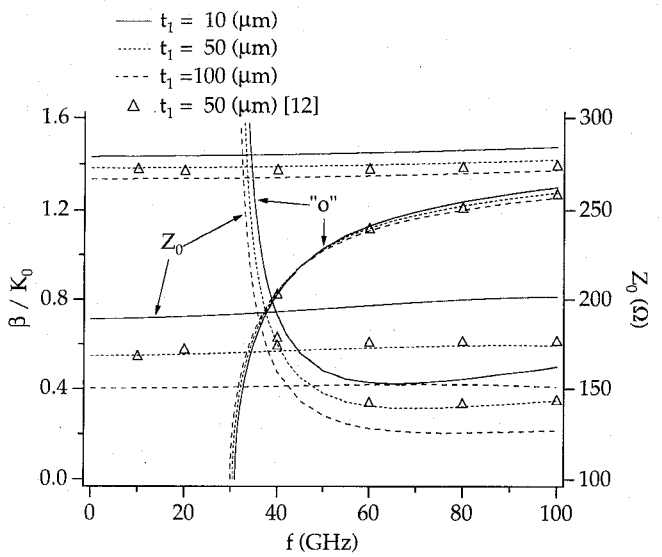

Fig. 3. Normalized propagation constants and characteristic impedance of even- and odd-modes versus frequency for different metallization thickness in coupled slotline: $a = b = 1.55$ mm, $h_1 + t_1 = h_2 = 1.44$ mm, $w = s = 0.2$ mm, $d = 0.22$ mm, $t_2 = e = c = 0$ mm, $\varepsilon_r = 3.75$, "o" stands for the odd-mode.

expansions are only related to the subregions encompassing the symmetric plan except the finite conductor thickness gaps (II).

With the help of the conventional spectral-domain analysis, two matrix equations which relate the tangential electric fields to the magnetic counterparts at lower and upper boundary apertures are obtained, such that

$$\begin{pmatrix} \tilde{H}_x^- \\ -\tilde{H}_z^- \end{pmatrix}_n^i = \frac{1}{j\omega\mu_0\gamma} \begin{bmatrix} \gamma^2 - \beta^2 & -\alpha\cdot\beta \\ -\alpha\cdot\beta & \gamma^2 - \alpha^2 \end{bmatrix}_n^i \cdot \left\{ \frac{1}{th(\gamma\cdot h)} \begin{pmatrix} \tilde{E}_z^- \\ \tilde{E}_x^- \end{pmatrix} - \frac{1}{sh(\gamma\cdot h)} \begin{pmatrix} \tilde{E}_z^+ \\ \tilde{E}_x^+ \end{pmatrix} \right\}_n^i \tag{4}$$

and

$$\begin{pmatrix} \tilde{H}_x^+ \\ -\tilde{H}_z^+ \end{pmatrix}_n^i = \frac{1}{j\omega\mu_0\gamma} \begin{bmatrix} \gamma^2 - \beta^2 & -\alpha\cdot\beta \\ -\alpha\cdot\beta & \gamma^2 - \alpha^2 \end{bmatrix}_n^i \cdot \left\{ \frac{1}{sh(\gamma\cdot h)} \begin{pmatrix} \tilde{E}_z^- \\ \tilde{E}_x^- \end{pmatrix} - \frac{1}{th(\gamma\cdot h)} \begin{pmatrix} \tilde{E}_z^+ \\ \tilde{E}_x^+ \end{pmatrix} \right\}_n^i \tag{5}$$

where the superscripts $(-)$ and $(+)$ denote the lower and upper apertures.

In the space domain, the tangential electric and magnetic fields should satisfy the boundary and continuity conditions at interfaces. On the basis of the complementary property between $\vec{E}_t$ and $\vec{J}_t$ at interfaces, the power conservation in the transverse direction should hold, which is determined by the following equation:

$$\int (\vec{E}_t^- \times \vec{H}_t^{-^*}) \cdot dx = \int (\vec{E}_t^+ \times \vec{H}_t^{+^*}) \cdot dx. \tag{6}$$

Invoking Parseval's theorem in (6) and substituting (4) and (5) into (6), a set of linear homogeneous equations is derived. Propagation constant β can be obtained simply through the application of Galerkin's technique.

In spectral domain analysis, the selection of basis function is important in order to obtain effective numerical computation. Following the work in [16], [17], the tangential electric fields at interfaces in Fig. 2 are expanded in terms of the functions

$$\begin{bmatrix} E_x \\ E_z \end{bmatrix} = \sum_{m=1}^{N} \frac{1}{\sqrt{1 - \left(\frac{x}{w/2}\right)^2}} \cdot \begin{bmatrix} C_{xm} \cdot \cos\left[\frac{m-1}{2}\pi\left(\frac{x}{w/2} - 1\right)\right] \\ C_{zm} \cdot \sin\left[\frac{m-1}{2}\pi\left(\frac{x}{w/2} - 1\right)\right] \end{bmatrix} \tag{7}$$

for coupled slot and

$$\begin{bmatrix} E_x \\ E_z \end{bmatrix} = \sum_{l=1}^{L} \frac{1}{\sqrt{1 - \left(\frac{x}{w_1/2}\right)^2}} \cdot \begin{bmatrix} D_{xl} \cdot \cos\left[(m-k_0)\pi\left(\frac{x}{w_1/2} - 1\right)\right] \\ D_{zl} \cdot \sin\left[(m-k_0)\pi\left(\frac{x}{w_1/2} - 1\right)\right] \end{bmatrix} \tag{8}$$

for pedestal or septumin in which $k_0 = 0.5$ and 1 for the even and odd modes, respectively. It should be noted that the first term of E_z in (7) and (8) for odd-mode is equal to zero and it is not included in numerical computations. However, it yields a better presentation for the number of basis function considered in the analysis. Characteristic impedances based on the voltage-power definition are calculated for design consideration [18].

III. Results

To examine the accuracy of the proposed method, Fig. 3 shows frequency-dependent normalized propagation constants and characteristic impedance of both even- and odd-modes for conventional coupled slotlines with different thickness of metallization which denotes $t_1 = 10$, 50, and 100 μm. Our results promise a good agreement with those obtained in [12] using the mode-matching method with conservation of complex power technique. The results indicate that the metallization thickness has a significant effect on the propagation characteristics of the fundamental modes.

Fig. 4 illustrates the effect of the mountings with and without pedestal on the normalized propagation constant and characteristic impedance for the even- and odd-modes as a function of frequency in coupled slotline. It is observed that the effect of choosing different mounting on the even-mode is not significant. This can well be explained by the fact that the field of the even-mode is mainly restricted around the slot region. At low frequencies, the effect of the pedestal mounting on even-mode is more visible than that of the inverse pedestal. At higher frequencies beyond 22 GHz as shown in the figure, the characteristic impedance of the pedestal

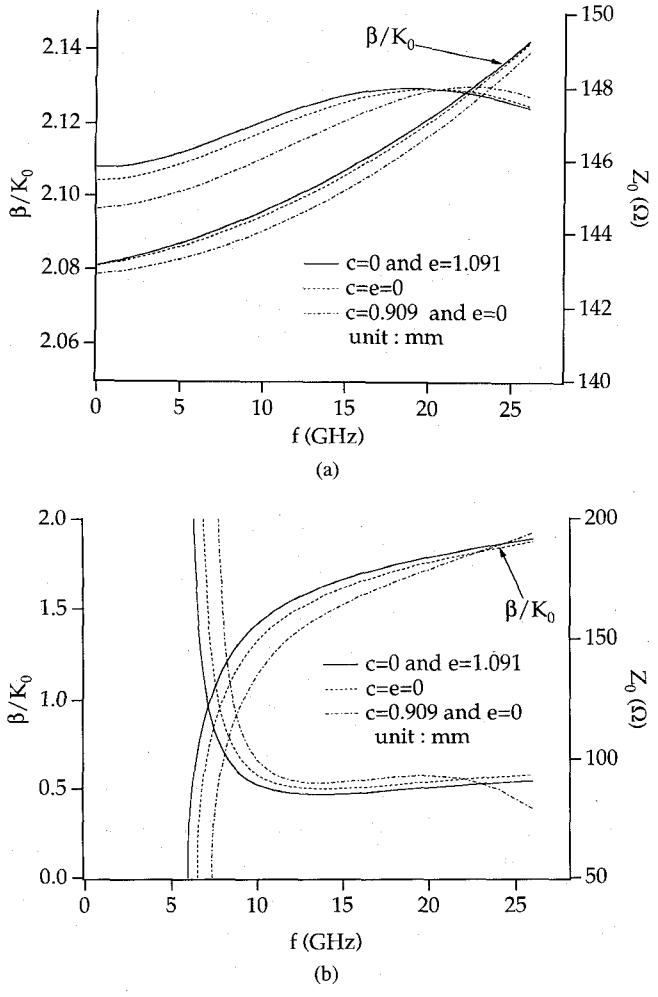

Fig. 4. Dispersion characteristics and characteristic impedance in coupled slotline with and without pedestals: $a = 4.318$ mm, $h_1 = 5.0$ mm, $h_2 = 5.1$ mm, $w = 0.4$ mm, $s = 0.2$ mm, $d = 0.5$ mm, $t_1 = 50$ μm, $t_2 = 0$ mm, $\varepsilon_r = 9.8$. (a) Even mode. (b) Odd mode.

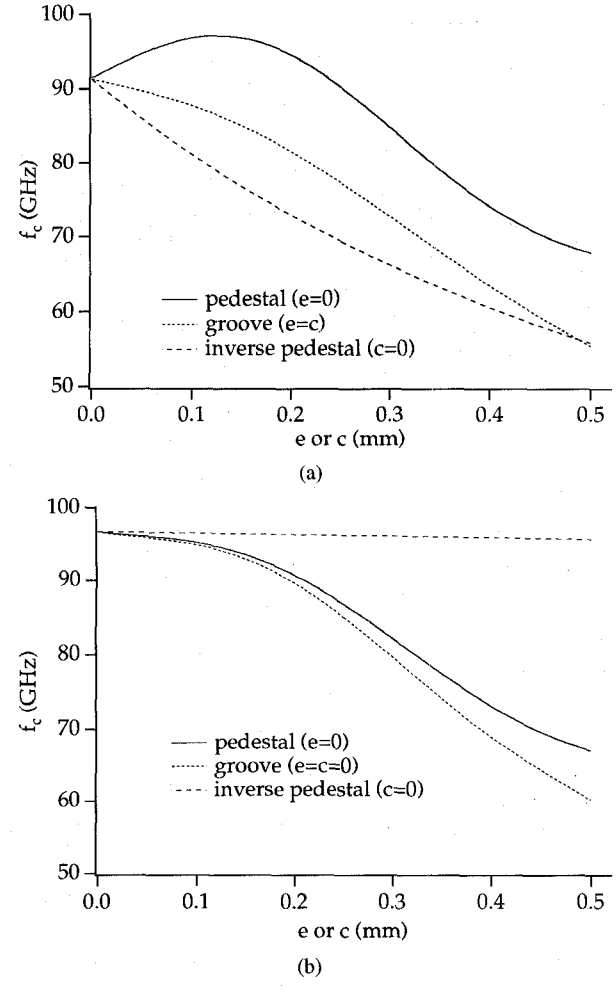

Fig. 6. Effect of three suspended mountings on cutoff frequencies of the first higher-order even- and odd-modes in coupled slotline: $a = 1.55$ mm, $h_1 = 1.5$ mm, $h_2 = 1.33$ mm, $w = s = 0.2$ mm, $d = 0.22$ mm, $t_1 = 50$ μm, $t_2 = 0$ mm, $\varepsilon_r = 3.75$. (a) Even mode. (b) Odd mode.

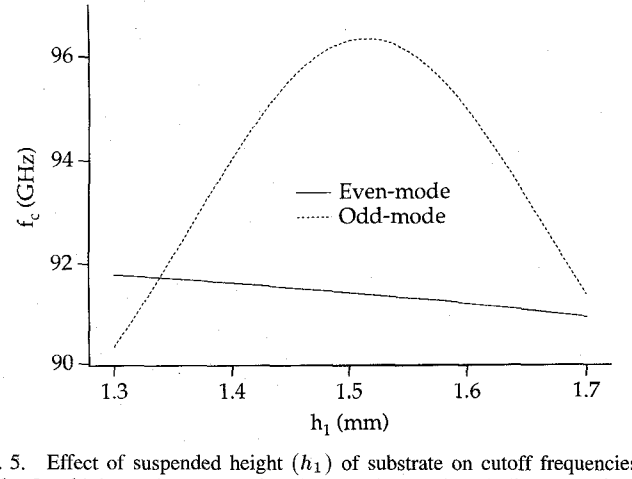

Fig. 5. Effect of suspended height (h_1) of substrate on cutoff frequencies of the first higher-order even-and odd-modes in coupled slotline: $a = b = 1.55$ mm, $h_1 + h_2 = 2.845$ mm, $w = s = 0.2$ mm, $d = 0.22$ mm, $t_1 = 35$ μm, $t_2 = e = c = 0$ mm, $\varepsilon_r = 3.75$.

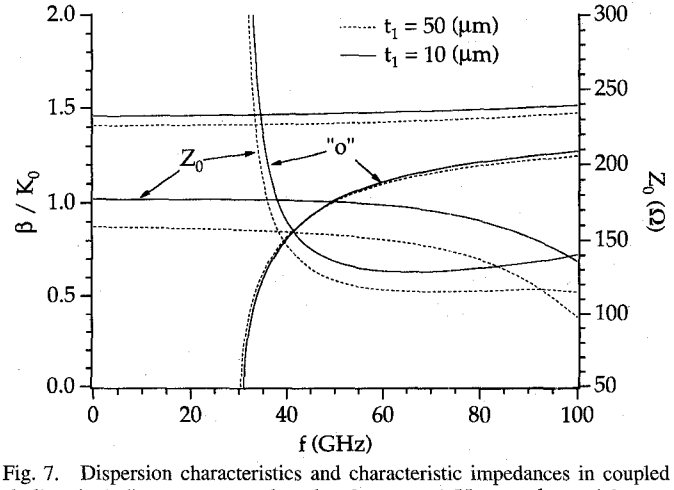

Fig. 7. Dispersion characteristics and characteristic impedances in coupled slotline including septum and pedestal: $a = 1.55$ mm, $b = 1.2$ mm, $t_1 = t_2, d = 0.22$ mm, $h_1 + t_1 = h_2 + t_2 = 1.44$ mm, $w = s = 0.2$, $w_1 = 0.6$ mm, $\varepsilon_r = 3.75$.

mounting is slightly higher than that of the inverse pedestal mounting. This is because the field is more confined toward the slot region with higher frequencies. As can be expected, the effect of various mounting schemes on the odd-mode is significant. At higher frequencies, the characteristic impedance of the pedestal mounting is lower than that of its counterparts while its normalized propagation constant is higher. This phenomenon can also be attributed to the interaction among

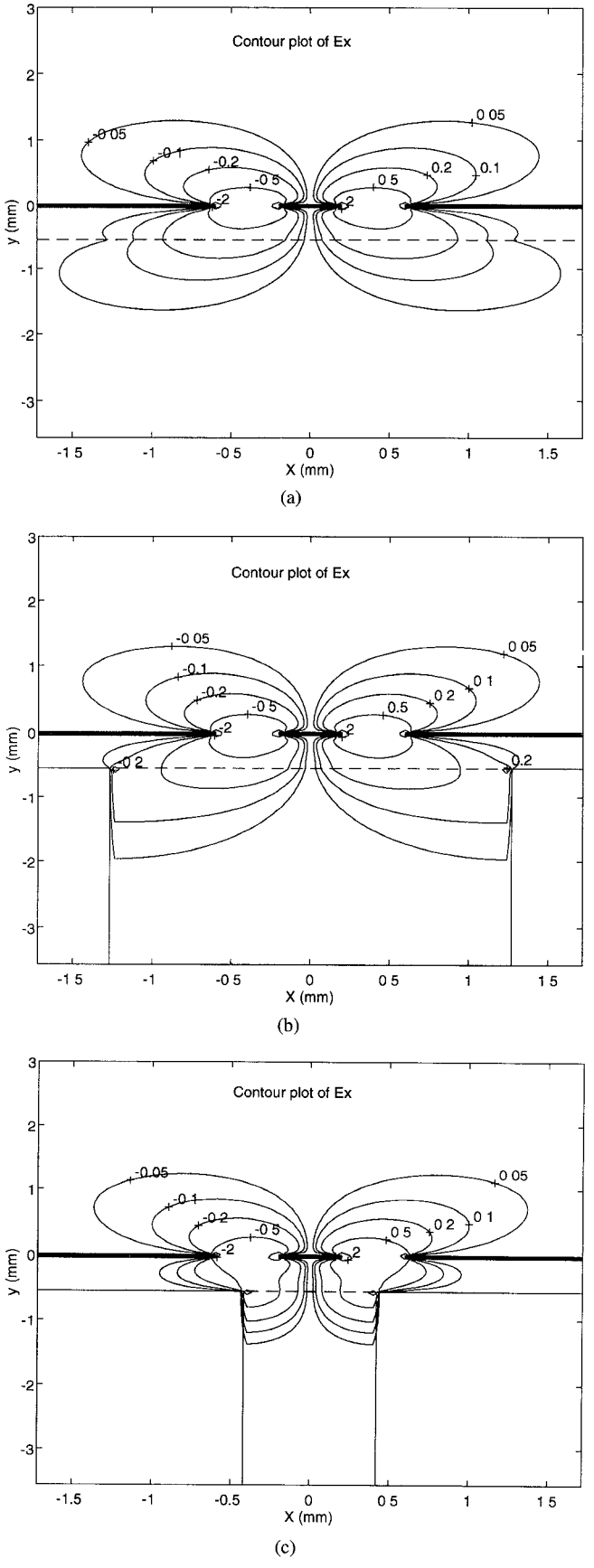

Fig. 8. Contour plot of E_x for the even-mode in coupled slotlines with and without pedestals: $a = 4.318$ mm, $h_1 = 5.0$ mm, $h_2 = 5.1$ mm, $w = s = 0.4$ mm, $d = 0.5$ mm, $t_1 = 50$ μm, $t_2 = e = 0$ mm, $\varepsilon_r = 9.8$, $f = 12$ GHz. (a) $c = 0$ mm, (b) $c = 0.909$ mm, and (c) $c = 1.759$ mm.

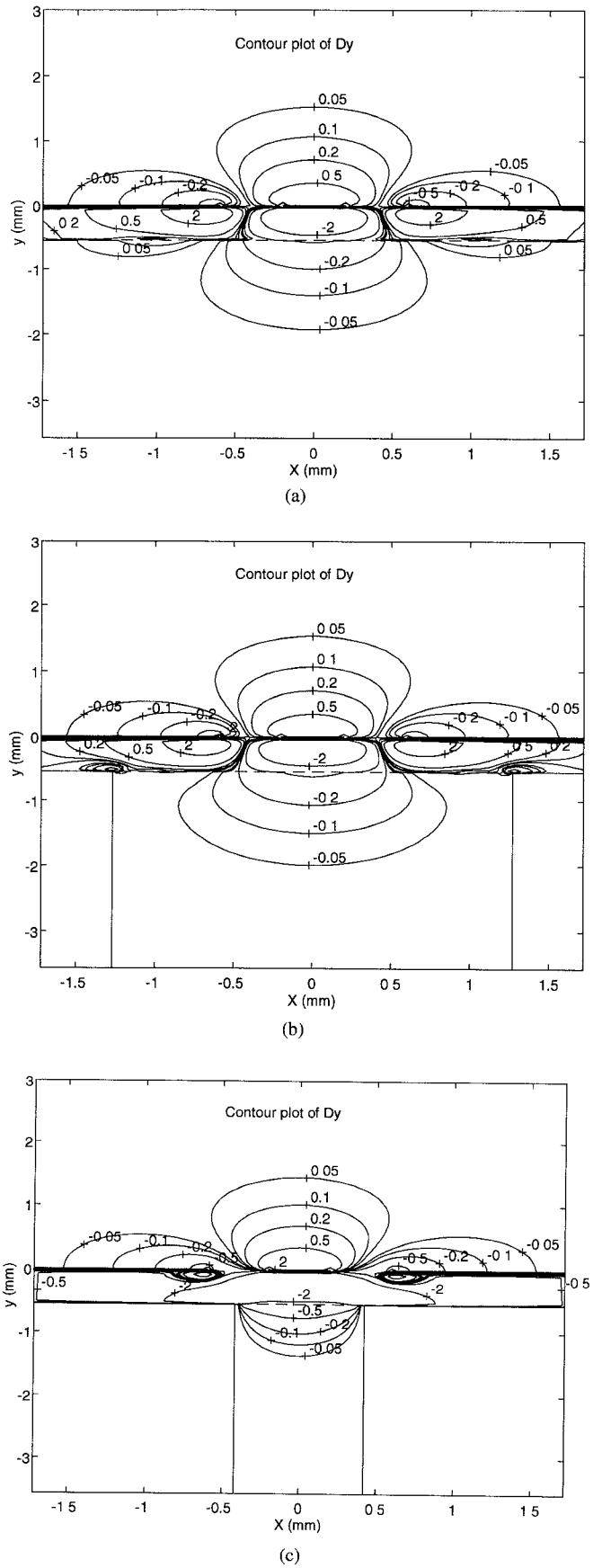

Fig. 9. Contour plot of D_y for the even-mode in a coupled slotline with and without pedestals: the structure parameters and frequency is referred as to Fig. 8.

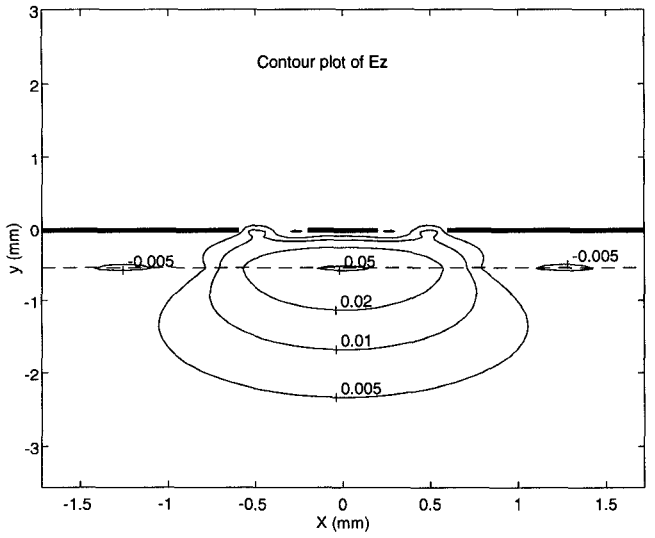

(a)

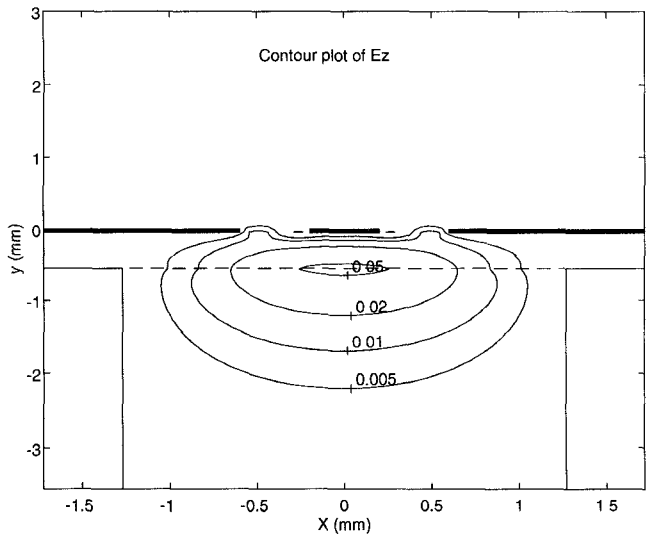

(b)

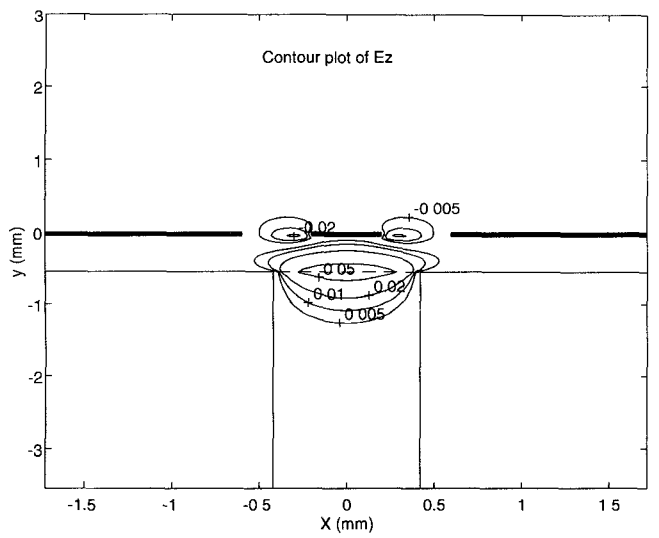

(c)

Fig. 10. Contour plot of E_z for the even-mode in a coupled slotline with and without pedestals: the structure parameters and frequency is referred as to Fig. 8.

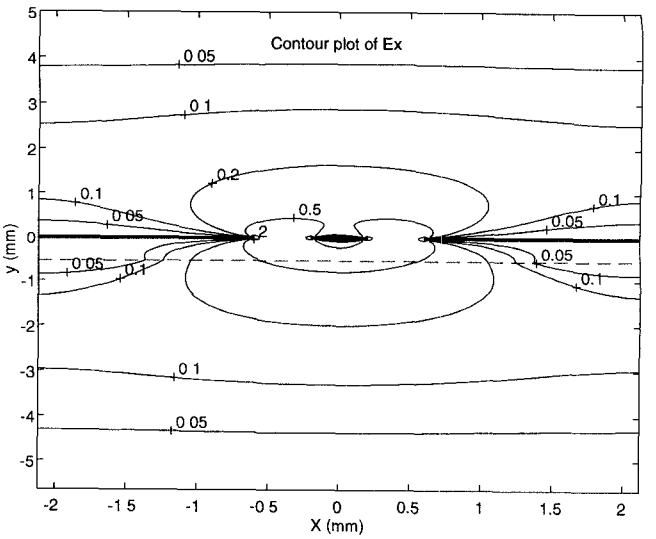

(a)

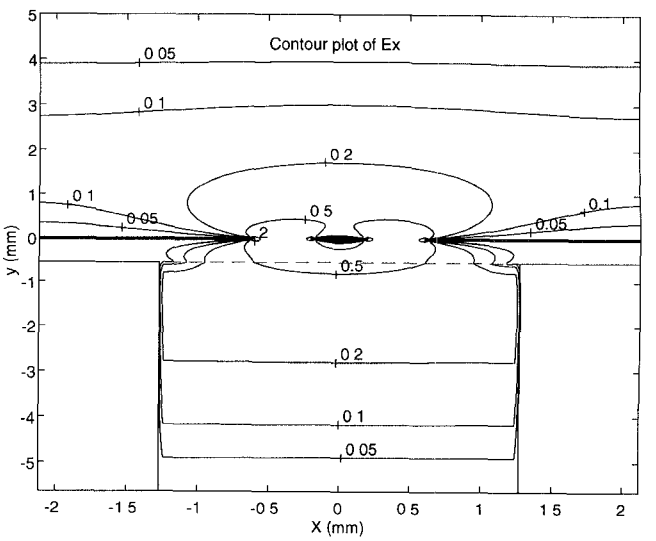

(b)

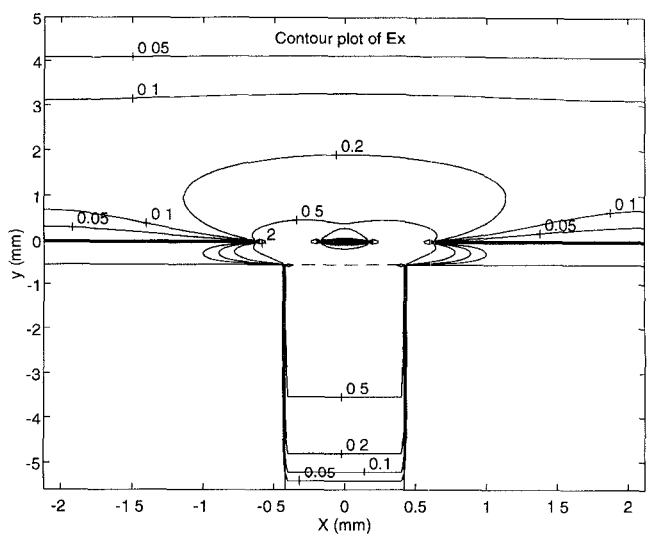

(c)

Fig. 11. Contour plot of E_x for the odd-mode in a coupled slotline with and without pedestals: the structure parameters and frequency is referred as to Fig. 8.

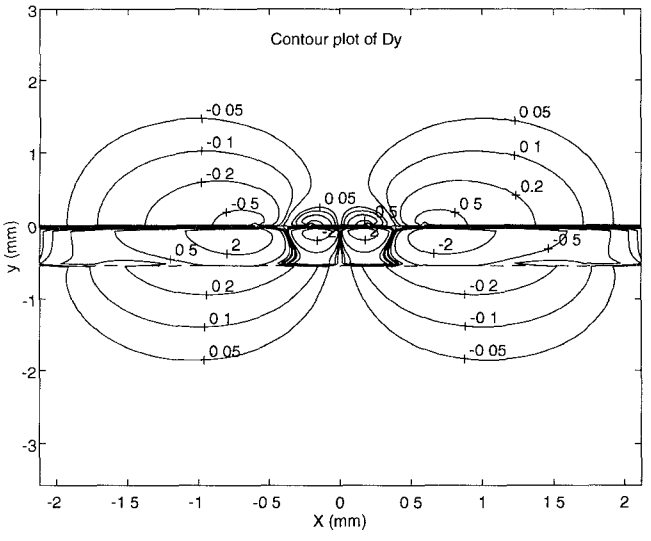

(a)

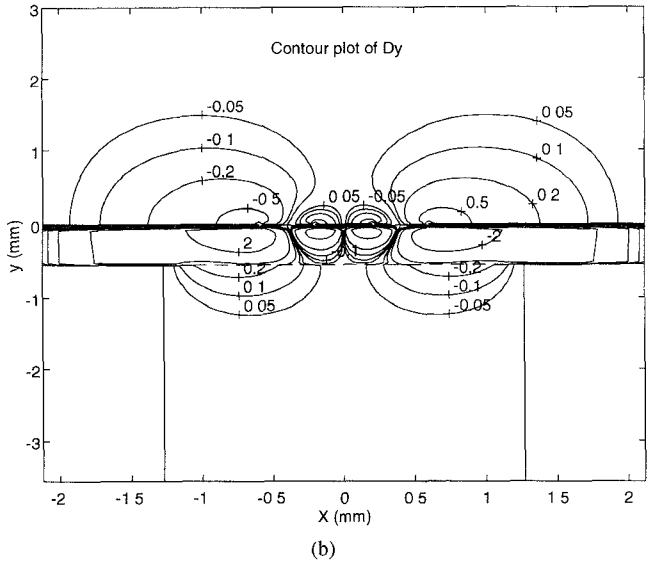

(b)

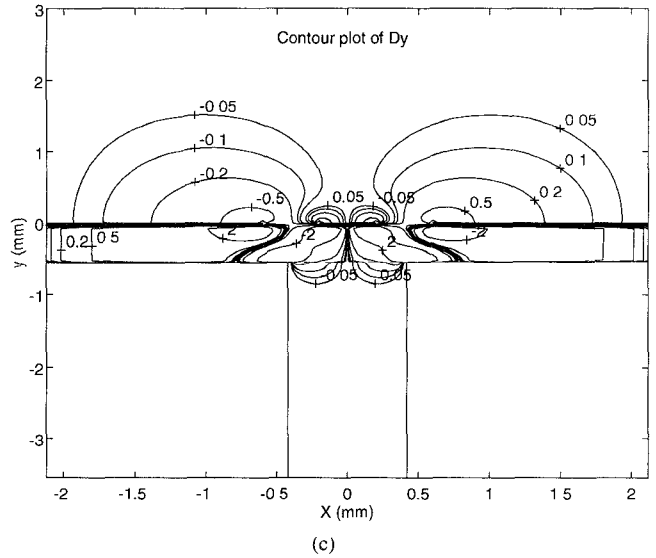

(c)

Fig. 12. Contour plot of D_y for the odd-mode in a coupled slotline with and without pedestals: the structure parameters and frequency is referred as to Fig. 8.

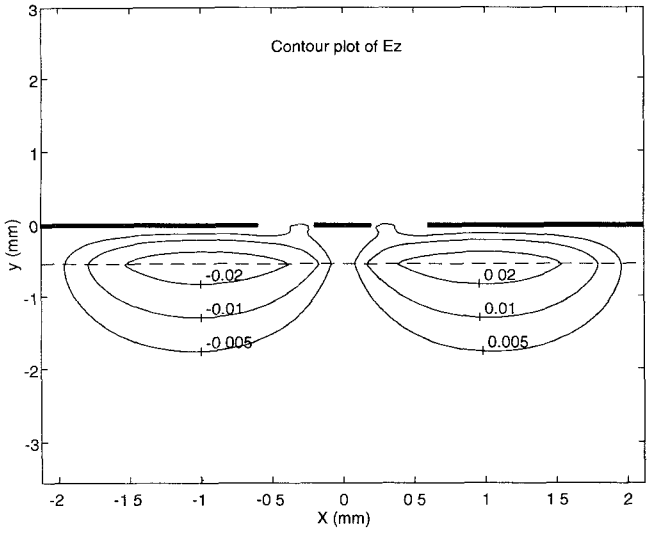

(a)

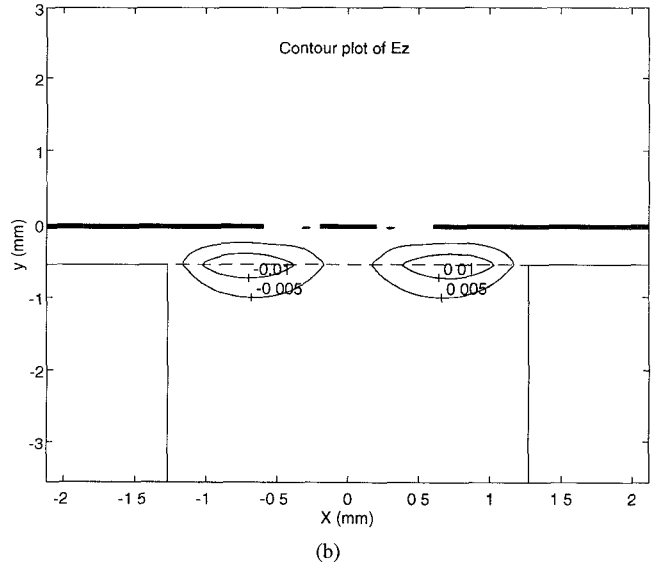

(b)

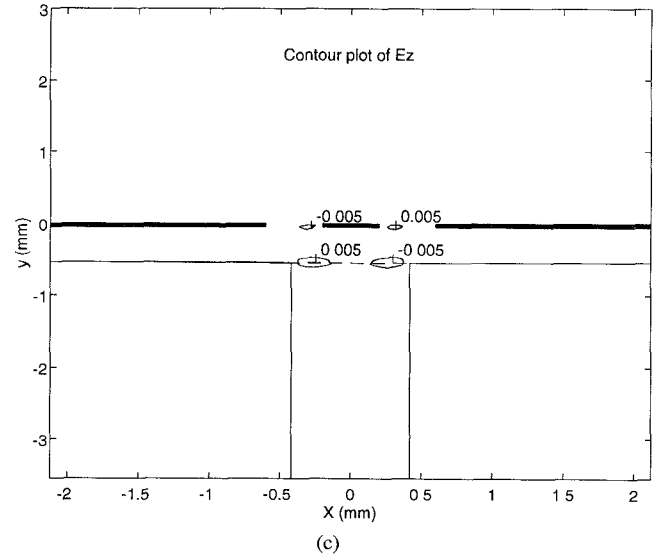

(c)

Fig. 13. Contour plot of E_z for the odd-mode in a coupled slotline with and without pedestals: the structure parameters and frequency is referred as to Fig. 8.

various modes. For the pedestal mounting, such an interaction is more pronounced, particularly when the distance between pedestals is small.

Fig. 5 shows the effect of the suspended height on the cutoff frequencies of first higher-order even- and odd-modes. As the suspended height varies under the condition of $h_1 + h_2$ = constant, the cutoff frequency of the first higher-order even-mode slightly decrease while that of the odd-mode is significantly affected and a maximum value of $f_c = 96.6$ GHz is attained around $h_1 = 1.5$ mm that corresponds to the middle of the shielded rectangular enclosure. In the coupled slotline, the field of the odd-mode is spread over in the structure. The influence of three mounting geometries on the first higher-order even- and odd-modes is depicted in detail in Fig. 6. The cutoff frequencies of the first higher-order even-mode for the inverse pedestal and the groove mounting decrease as the mounting sizes increase. However, the cutoff frequency for the pedestal mounting increases at first and begins to decrease around $c = 0.12$ mm. This may be explained by the fact that, for a larger pedestal (small c), in addition to the expected strong field concentration in slots, a certain portion of the tangential electric field of the even-mode is also located between the central conductor and the 90° edge of the pedestal and thus increases overall capacitive effect similar to H-plane ridge waveguide. However, this effect tends to be negative as long as the distance between pedestals becomes small. This is because the normal (vertical) electric field appears to be dominant over its tangential counterpart. As a result, there is an optimum choice of the pedestal for wideband applications. The effect of mounting geometries on the cutoff frequency of the first higher odd-mode is significantly different from that on its even counterpart. The cutoff frequency of the first higher-order odd-mode for the inverse pedestal mounting is insensitive to the mounting size. This is attributed to the fact that the field of the odd-mode, though its loose distribution, is mainly limited by a certain region that is related to the slots.

Fig. 7 shows dispersion characteristics of the normalized propagation constant and characteristic impedance of the fundamental modes for a coupled slotline with both septum and pedestal considering different metallization thickness. The effect of the septum on propagation characteristics is similar to pedestal in this case. It is found that, indeed, the compensation due to the septum introduces an additional degrees of freedom for design consideration.

To understand better the propagation mechanism and influence of pedestals on the fundamental modes, the electric field contours are plotted in the whole cross-section. Figs. 8–10 show the effect of pedestal positions on the electric fields in the case of the even-mode. It is vividly observed that the field under the slots tends to be more compressed with decreasing the distance between the pedestals. Nevertheless, the field above the slots remains nearly unchanged. This clearly indicates that the coplanar waveguide mode converts gradually into a hybrid microstrip-coplanar waveguide mode. In practical applications, it is therefore important that the field profile at the launching probe or connector should be matched to the desired mode, and the conventional concept on the impedance matching is no longer complete for hybrid mode circuits. It should be noted that the electric flux density D_y is plotted instead of E_y due to the field continuity condition for a better presentation. In Fig. 10, it can be seen that E_z is negligible compared to the other fields, confirming the validity of quasi-static analysis at low frequencies. The field profiles for the odd-mode are presented in the Figs. 11–13. This once again confirms the above discussion that the odd-mode fields are spread over the whole structure. Nevertheless, the fields around the slot regions are still dominant. This fact indicates that the effect of the inverse pedestal mounting scheme on the characteristics of the odd-mode is insensitive.

IV. Conclusion

In this work, the coupled slotlines with various suspended mounting geometries considering finite thickness of planar conductors are analyzed by a recently developed enhanced spectral-domain method. Propagation characteristics and electrical properties of coupled slotline are discussed in detail for wideband applications and design consideration. Influences and features in terms of different mounting schemes are demonstrated for the normalized propagation constant, the characteristic impedance and the cutoff frequency of the first higher-order modes (the even- and odd-modes). The field profiles of the fundamental modes in coupled slotline with pedestals are plotted. The proposed enhanced SDA proves to be a powerful technique to model a class of complex planar structures, thereby offering efficient analysis and accurate design of MIC's for microwave and millimeter-wave applications.

References

[1] M. Muraguchi, T. Hirota, A. Minakawa, K. Ohwada, and T. Sugeta, "Uniplanar MMIC's and their applications," *IEEE Trans. Microwave Theory Tech.*, vol. MTT-36, pp. 1896–1901, Dec. 1988.

[2] C. Ho, L. Fan, and K. Chang, "Broad-band uniplanar hybrid-ring and branch-line couplers," *IEEE Trans. Microwave Theory Tech.*, vol. MTT-41, pp. 2116–2124, Dec. 1993.

[3] T. Itoh, "Overview of quasi-planar transmission lines," *IEEE Trans. Microwave Theory Tech.*, vol. MTT-37, pp. 275–280, Feb. 1989.

[4] M. Riaziat, R. Majidi-Ahy, and I. J. Feng, "Propagation modes and dispersion characteristics of coplanar waveguides." *IEEE Trans. Microwave Theory Tech.*, vol. MTT-38, pp. 245–251, Mar. 1990.

[5] M. Naghed and I. Wolff, "Equivalent capacitances of coplanar wave guide discontinuities and interdigitated capacitors using a 3-dimensional finite difference method," *IEEE Trans. Microwave Theory Tech.*, vol. MTT-38, pp. 1805–1815, Dec. 1990.

[6] F. Alessandri, G. Baini, M. Mongiardo, and R. Sorrentino, "3-D mode matching technique for the efficient analysis of coplanar MMIC discontinuities wit finite metallization thickness," *IEEE Trans. Microwave Theory Tech.*, vol. MTT-41, pp. 1625–1629, Sept. 1993.

[7] H. Shigesawa, M. Tsuji, and A. A. Oliner, "Conductor-backed slot line and coplanar waveguide: Dangers and full-wave analysis," in *IEEE MTT-s Int. Microwave Symp. Dig.*, 1988, pp. 199–202.

[8] ——, M. Tsuji, and A. A. Oliner, "A new mode-coupling effect on coplanar waveguide s of finite width," in *IEEE MTT-s Int. Microwave Symp. Dig.*, 1990, pp. 1063–1066.

[9] R. W. Jackson, "Mode conversion at discontinuities in finite-width conductor-backed coplanar waveguide," *IEEE Trans. Microwave Theory Tech.*, vol. MTT-37, pp. 1582–1589, Oct. 1989.

[10] K. Wu, R. Vahldieck, J. L. Fikart, and H. Minkus, "The influence of finite conductor thickness and conductivity on fundamental and higher-order modes in miniature hybride MIC's (MHMIC's) and MMIC's," *IEEE Trans. Microwave Theory Tech.*, vol. MTT-41, pp. 421–430, Mar. 1993.

[11] W. T. Lo *et al.*, "Resonant Phenomena in conductor-backed coplanar waveguides (CBCPW's)," *IEEE Trans. Microwave Theory Tech.*, vol. MTT-41, pp. 2099–2107, Dec. 1993.
[12] R. R. Mansour and R. H. Macphie, "A unified hybrid-mode analysis for planar transmission lines with multilayer isotropic/anisotropic substrates," *IEEE Trans. Microwave Theory Tech.*, vol. MTT-35, pp. 1382–1391, Dec. 1987.
[13] T. Wang and Z. Sun, "Analysis of novel wideband ridge-loaded finline including finit metallisation thickness and substrate mounting grooves," *Electron. Lett.*, vol. 28, no. 25, pp. 2356–2357, Dec. 1992.
[14] T. Wang and K. Wu, "Enhanced spectral domain analysis of coupled slotlines with septum and pedestal considering finite thickness of conductors for wideband MIC's," in *IEEE MTT-s Int. Microwave Symp. Dig.*, 1994, pp. 1037–1040.
[15] ——, "An efficient approach to modeling of quasi-planar structures using the formulation of power conservation in spectral domain," *IEEE Trans. Microwave Theory Tech.*, vol. 43, pp. 1136–1143, May 1995.
[16] R. Jansen, "Unified user-oriented computation of shielded, covered and open planar microwave and millimeter-wave transmission-line characteristics," *Microwave Opt. Acoust.*, vol. 3, pp. 14–22, Jan. 1979.
[17] T. Itoh, "Sectral-domain immittance approach for dispersion characteristics of generalized printed transmission lines," *IEEE Trans. Microwave Theory Tech.*, vol. MTT-28, pp. 733–736, July 1980.
[18] J. Bornemann and F. Arndt, "Calculating the characteristic impedance of finlines by transverse resonance method," *IEEE Trans. Microwave Theory Tech.*, vol. MTT-34, pp. 85–92, Jan. 1986.

Tongqing Wang was born in Jiangsu, China. He received the B.Eng. and M.Eng. degrees in Radio Engineering from Southeast University, Nanjing, People's Republic of China, in 1984 and 1989, respectively.

He joined the faculty at Southeast University in 1984, where he conducted research in the areas of numerical modeling of planar integrated circuits, microwave and millimeter-wave components, and millimeter-wave quasi-optical technology. Since 1993, he has been working toward the Ph.D. degree in the Department of Electrical and Computer Engineering at Ecole Polytechnique, Montreal, Canada. His current research interests include numerical methods for electromagnetic field problems, CAD of microwave integrated circuits, planar and quasi-planar components for broadband communication applications, and high performance microwave circuits for wireless communications.

Ke Wu (M'87–SM'92) was born in Jiangsu, China. He received the B.Sc. degree (with distinction) in radio engineering from Nanjing Institute of Technology (now Southeast University), Nanjing, China, and the D.E.A. degree in electronics and Ph.D. degree (with distinction) in optics, optoelectronics, and microwave engineering from Institut National Polytechnique de Grenoble (INPG), France.

During the years 1983–1987, he conducted research in the Laboratoire d'Eléctromagnetisme, Microondes et Optoélectronics (LEMO), Grenoble, France. From March 1988 to January 1992 he was a research associate at the University of Victoria, Victoria, B.C., Canada. In February 1992, he joined the Département de génie électrique et de génie informatique at the École Polytechnique de Montréal as an assistant professor. His main research interests include analysis and design of various microwave/millimeter-wave integrated circuits and antennas, high-speed interconnects and packaging effects, numerical methods, dielectric material characterizations and superconducting devices. He is also interested in research and design of broadband optoelectronic components and lightwave transmission systems with emphasis on traveling-wave electro-optic modulators, couplers, and switches. He has published more than 100 papers

Dr. Wu received a U.R.S.I. Young Scientist Award in 1987 and, together with two coauthors, the Oliver Lodge Premium from the IEE in 1988. He serves on the editorial or review boards of various technical journals.